The marine bacterium Marinobacter hydrocarbonoclasticus SP17 degrades a wide range of lipids and hydrocarbons through the formation of oleolytic biofilms with distinct gene expression profiles.

Julie Mounier, Arantxa Camus, Isabelle Mitteau, Pierre-Joseph Vaysse, Philippe Goulas, Régis Grimaud, Pierre Sivadon

TITLE PAGE

The marine bacterium *Marinobacter hydrocarbonoclasticus* SP17 degrades a wide range of lipids and hydrocarbons through the formation of oleolytic biofilms with distinct gene expression profiles.

Authors

Julie MOUNIER, Arantxa CAMUS, Isabelle MITTEAU, Pierre-Joseph VAYSSE, Philippe GOULAS, Régis GRIMAUD, Pierre SIVADON

Affiliations

Université de Pau et des Pays de l'Adour, Equipe Environnement et Microbiologie, UMR UPPA-CNRS 5254 IPREM, IBEAS - BP1155, 64013 Pau Cedex, France

Corresponding author: Pierre SIVADON

Université de Pau et des Pays de l'Adour, Equipe Environnement et Microbiologie, UMR UPPA-CNRS 5254 IPREM, IBEAS - BP1155, 64013 Pau Cedex, France

pierre.sivadon@univ-pau.fr; tel: +33 559 407 473; FAX: +33 559 407 494

Keywords: Carbon cycle; oceans; degradation of hydrophobic organic carbon; Transcriptome;

Running title: Gene expression in a microbial biofilm degrading oily carbon

ABSTRACT

Hydrophobic organic compounds (mainly lipids and hydrocarbons) represent a significant part of the organic matter in the marine waters and their degradation has thus an important impact in the carbon fluxes within the oceans. However, because they are nearly insoluble in the water phase, their degradation by microorganisms occurs at the interface with water therefore requiring specific adaptations like biofilm formation. We show that *Marinobacter hydrocarbonoclasticus* SP17 develops biofilms, referred as oleolytic biofilms, on a larger variety of hydrophobic substrates than suspected before, including hydrocarbons, fatty alcohols, fatty acids, triglycerides and wax esters. A microarray analysis confirmed that biofilm growth on *n*-hexadecane or triolein involved distinct genetic responses together with a core of common genes that might concern general mechanisms of biofilm formation. Biofilm growth on triolein modulated the expression of hundreds of genes in comparison to *n*-hexadecane. Processes related to primary metabolism and genetic information processing were down-regulated. Most of the genes over-expressed on triolein had unknown function. Surprisingly, their genome localization is restricted to a few regions identified as putative genomic islands or mobile elements. These results are discussed with regard to the adaptive responses triggered by *M. hydrocarbonoclasticus* SP17 to occupy a specific niche in marine ecosystems.

INTRODUCTION

Hydrophobic organic compounds (HOCs), which include lipids and hydrocarbons, are ubiquitous in the marine environment. Their hydrophobic properties make them virtually absent in the water phase. They are rather represented in the particulate phase as living organisms, cell compartments such as membranes or carbon storage bodies, non-aqueous liquid, adsorbed onto inorganic or organic surfaces or embedded in organic gels. Lipids account for about 15% of the organic matter in the euphotic zone in equatorial oceans (Wakeham *et al*., 1997). They are among the most labile organic compounds in oceans since they are almost completely degraded in the upper 100 m of the ocean, entailing that some bacteria are able to degrade them efficiently (Wakeham *et al*., 1997; Yoshimura & Hama, 2012). Considering that microorganisms are believed to take up substrates only as water-dissolved molecules, this suggests that some heterotrophic bacteria may have developed efficient strategies to adhere to these hydrophobic interfaces, to solubilize and transport hydrophobic substrates, making them more bioavailable (Harms *et al*., 2010a).

To date, the characterization of marine bacterial species specialized in the degradation of HOCs has mostly been being focused on hydrocarbon-degrading capabilities as they respond to social concerns towards pollution of marine environments. These studies have put forward bacterial species highly specialized in hydrocarbon degradation, referred to as the marine hydrocarbonoclastic bacteria (Yakimov *et al*., 2007). These bacteria belong to only few genera like *Alcanivorax, Cycloclasticus, Oleiphilus, Oleispira* and *Thallassolituus*. However, their high substrate specificity doesn't likely involve them in the recycling of lipids produced in the euphotic zone of oceans.

In contrast to terrestrial hydrocarbon degraders which tend to be metabolically versatile (Mara *et al*., 2012), descriptions of marine bacteria able to degrade a wide range of lipids and hydrocarbons, are very rare in the literature (Golyshin *et al*., 2002; Klein *et al*., 2008; Tanaka

et al., 2010). *Marinobacter hydrocarbonoclasticus* SP17 was initially described as an hydrocarbonoclastic bacterium isolated from oil-contaminated marine sediment (Gauthier *et al*., 1992). This bacterium was further shown to form biofilms at the interface between water and *n*-alkanes (C_8 to C_{28}) or metabolizable *n*-alcohols (C_{12} and C_{16}) (Klein *et al*., 2008; Vaysse *et al*., 2009; Grimaud *et al*., 2012). *M. hydrocarbonoclasticus* SP17 forms biofilms only on substrates that it can metabolize. No biofilm is observed on non-metabolizable HOCs like branched alkanes (Klein *et al*., 2008). This substrate specificity suggests that biofilm formation is determined by the presence of a nutritive interface. Furthermore, the rate of *n*-hexadecane degradation dramatically decreases when the biofilm is disorganized, thus confirming that biofilm formation may constitutes an efficient adaptive strategy for assimilating hydrocarbon (Klein *et al*., 2008). Such biofilms, which have been observed with many strains or consortia degrading aliphatic or aromatic hydrocarbons, are thought to provide bacteria with efficient mechanisms to access hydrocarbons. In a few examples, they have been shown to increase the rate of mass transfer of hydrocarbons by reducing the diffusion path of the substrate (Golyshin *et al.*, 2002; Johnsen *et al*., 2005; Grimaud, 2010; Harms *et al*., 2010b; Jiménez *et al*., 2011; Jung *et al*., 2011; Notomista *et al*., 2011; Tribelli *et al*., 2012). A proteomic study was conducted on the *M. hydrocarbonoclasticus* SP17 biofilm growing on *n*-hexadecane (Vaysse *et al*., 2009). It revealed that biofilm cells expressed a specific proteome in which 50% of the detected proteins had their quantity levels altered when compared to planktonic cells growing exponentially on acetate. The adaptation to alkane utilization as a carbon and energy source therefore involves a global change in cell physiology.

We have conducted a phenotypic study which shows that *M. hydrocarbonoclasticus* SP17 can grow a biofilm on a larger variety of HOCs than suspected in the previous studies. This result makes *M. hydrocarbonoclasticus* SP17 one of the first marine bacterial strains that degrade

both hydrocarbons and lipids. To obtain a more comprehensive picture of biofilm development on diverse HOCs, we have compared whole-genome transcriptomic data obtained from *M. hydrocarbonoclasticus* SP17 biofilms growing on *n*-hexadecane or triolein and from planktonic cells growing exponentially on acetate. Gene expression patterns confirmed that biofilm growth on either HOCs involved distinct genetic responses together with a core of common genes that might concern general mechanisms of biofilm formation. Taken together, the results presented in this paper shed light on bacterial cellular processes that may play a significant role in the recycling of a large fraction of the organic matter in the oceans.

MATERIALS AND METHODS

Bacterial strain and growth assays

The *Marinobacter hydrocarbonoclasticus* SP17 (ATCC 49840) strain was initially described by Gauthier *et al*. (1992). *M. hydrocarbonoclasticus* SP17 was currently cultivated in synthetic seawater (SSW) supplemented with 20 mM Na acetate (further referred as SSW acetate medium) as described by Klein *et al*. (2008). The *M. hydrocarbonoclasticus* MJ6-1 fluorescent strain derives from the SP17 strain. It was obtained by transformation of the spontaneous streptomycin-resistant JM1 strain (*rpsL*K58T, Sm^R) with the pUC18T-mini-Tn7T-Tp-eyfp plasmid (Choi & Schweizer, 2006, Mounier, 2013). The mini-Tn7 transposon integrated at the single Tn7 integration site of the *M. hydrocarbonoclasticus* SP17 genome (Grimaud *et al.*, 2012). This transposon expresses the eYFP fluorescent protein thanks to the modified *E. coli* lac operon promoter PA1/04/03.

Biofilm growth on HOC substrates that are solid at 30°C was tested in 24-wells polystyrene microplates (Evergreen Scientific). All chemicals were purchased from Sigma Aldrich.

Approximately 0.2 g of solid HOC were melted for 1 h at 90°C in wells and cooled at room temperature. Exponentially growing cells in SSW acetate were harvested by centrifugation at 10,000 g for 15 min at room temperature and suspended to a final OD_{600nm} of 0.1 in SSW medium. 1.5 mL of the cell suspension was added to each HOC-coated well and incubated at 30°C at 100 rpm. After 36 h of cultivation, the culture medium containing the planktonic cells was gently sucked out. Cells adhered to the solid substrate were stained for 3 min with 0.4 mL of crystal violet 1% (w/v). In these conditions, adhesion of cell to polystyrene wall compared to the HOC substrates was negligible. After 2 washes with MilliQ water, the crystal violet was extracted with 0.75 mL of acetic acid 10% (v/v) and ethanol 50% (v/v) and the absorbance was red at 595 nm. All measurements were repeated four times.

Biofilm growth on water insoluble HOC substrates that are liquid at 30°C was tested in 50 mL of SSW in 250-mL Erlenmeyer flasks at 30°C. Inoculation was carried out with exponentially growing cells in SSW acetate prepared as described above. Biofilm cultures on insoluble HOCs were gently shaken at 50 rpm. Biofilm quantities at the liquid-liquid interfaces were measured as described by Klein *et al.* (2008) after 24 h of cultivation.

Microscopy and imaging

Microscopic observations of *M. hydrocarbonoclasticus* biofilm cells were performed on MJ6-1 strain grown in the same conditions as those used to prepare RNAs for transcriptomics analyses, except that pyrene (Sigma Aldrich) was dissolved at 6 mg mL^{-1} in *n*-hexadecane or triolein prior to inoculation. Biofilm samples were mounted on glass slides and observations were made using an Axio Observer.Z1 inverted microscope (Zeiss, Germany) equipped with a 63x (Plan APO, N.A. 1.4, M 27) oil immersion lens. Differential interference contrast (DIC) observations were realized with the Zeiss PA 63x / 1.4 HR III optical component.

Epifluorescence microscopy was realized either by standard optical treatment or with the Zeiss ApoTome.2 attachment. Triolein or *n*-hexadecane particles stained with pyrene were visualized using epifluorescence illumination (excitation filter G365, Beamsplitter FT 395, emission BP 445/50). eYFP fluorescence was revealed with a BP 470/40 excitation filter, a Beamsplitter FT 495 and observed through a 445/50 emission filter. Images were acquired using a CCD Zeiss Axiocam 506 mono camera monitored by the Zeiss ZEN 2012 software. Image treatments were performed with ImageJ software (http://imagej.nih.gov/ij/).

RNA preparation and cDNA synthesis

Exponentially growing planktonic cells or biofilm samples were prepared as previously described (Vaysse *et al*., 2009). Total RNA from 50 mL of planktonic (DO_{600nm}~0.4) exponentially growing cells on SSW-acetate 20 mM or of biofilm cells from 300 mL-biofilm cultures in 500-mL Erlenmeyer flasks were isolated using the Extract-All kit (Eurobio). RNAs were extracted in triplicate from independent biological samples. Remaining traces of DNA were removed with DNAse I (Invitrogen) and DNAse-treated RNAs were immediately processed on RNA Easy Clean Up columns (Qiagen). RNA quality and quantity was checked with a RNA 600 Nano kit on a BioAnalyser 2100 (Agilent) and a Nanodrop ND-1000 Spectrophotometer (Labtech). Five µg of total RNAs were retro-transcribed using Superscript III enzyme and the first-strand cDNA synthesis kit (Invitrogen) using random hexamers. cDNAs were eventually purified using the MinElute Reaction Cleanup kit (Qiagen).

***M. hydrocarbonoclasticus* SP17 whole genome microarray design, hybridization and image acquisition**

The assembled whole genome sequence of *M. hydrocarbonoclasticus* SP17 was shared into 59 non-coding RNA sequences (tRNAs and rRNAs), 1,739 intergenic regions longer than 60

bp and 3,807 coding sequences (Grimaud *et al*., 2012). Probe design and microarray printing were performed by Roche NimbleGen. Six 45-60 mer oligonucleotides were designed for each of these genomic objects, three of them being in the forward sense and accompanied by their reverse complement (reverse strand). The oligonucleotides were chosen to span the 5' and 3' ends and an intermediate position. There were 182 genomic objects shorter than 300 bases for which only one or two probes could be selected (two or four probes if both strands are counted). Twenty-two groups of sequences sharing 100% of identity were represented by the same set of probes and three genes were not represented. All probes were synthesized in duplicate together with 6,186 random sequences with no similarity to any *M. hydrocarbonoclasticus* SP17 sequences, leading to 72,546 features per hybridization zone. The array design is available in the ArrayExpress database (www.ebi.ac.uk/arrayexpress) under accession number A-MEXP-2398. cDNA labeling, microarray hybridization and scanning were all performed at the BioChip Platform (Toulouse, France) according to Roche Nimblegen specifications.

Data processing and statistical analysis

Three arrays hybridized from three independent biological samples generated a total of 36 raw values for each genomic object in each growth condition. Raw microarray data are available in the ArrayExpress database under accession number E-MTAB-2593. Raw values obtained from intergenic sequences were not kept in the following analyses. Transcriptomic results were processed using the ANAIS software as follows (Simon & Biot, 2010). Array quality was assessed at the probe level. Robust Multi-Array Analysis background normalization and quantile normalization were performed for intra- and inter-array normalization, respectively (Bolstad *et al*., 2003; Irizarry *et al*., 2003). Gene expressions were summarized by median polish of the corresponding normalized probes set values. A total of 3,839 genes with signal

intensities above a 95% random threshold were kept for further studies. Gene differential expression (fold-change) was calculated as a ratio between normalized gene expression values for each experimental condition and the referent experimental condition. Significant fold-changes were statistically determined using an ANOVA-FDR adjusted *p*-value ≤ 0.05 (Benjamini & Hochberg, 1995).

The 'triangle plot' representation (Figure 3) of expression ratios reduced three-valued expression points (A, B, C) to two dimensions by plotting A/2 + B versus A/(A + B + C). Location in the plot is based on proportionality among expression levels, ignoring magnitude. Genes whose expression was high in one condition and low in the other two lie near a specific corner of the triangle, genes that were high in two conditions and low in the third are plotted along one edge of the triangle, and genes that were roughly equally expressed in all conditions fall toward the center. All analyses were performed in the R environment (http://www.r-project.org/) with the ADE4 package for construction of the triangle plots.

Sequence analysis and data mining

Biological interpretation of the transcriptomic datasets at the biological process level was carried out by mapping genes of the different expression categories in the KEGG pathway database (Kanehisa *et al*., 2013). Lists of genes downloaded in the "search&color" advanced mapping tool (http://www.genome.jp/kegg/tool/map_pathway1.html) and compared to the KEGG annotation of the *M. hydrocarbonoclasticus* SP17 genome available in the database. Whole genome alignments were performed with MAUVE 2.3.1 Java application using *M. hydrocarbonoclasticus* SP17 (GenBank ID: FO203363) and VT8 (formely *M. aquaolei* VT8, (Márquez & Ventosa, 2005)(GenBank ID: CP000514.1) full genome sequences downloaded from the NCBI Microbial Genomes database (http://www.ncbi.nlm.nih.gov/genome)(Darling *et al*., 2004). Alignments were performed using default settings. The putative genomic islands

in *M. hydrocarbonoclasticus* SP17 genome were predicted by an integrated method using IslandViewer program suite (Dhillon *et al*., 2013). Results were visualized with the DNAPlotter Java application of the Artemis genome viewer software (Carver *et al*., 2009). Results were exported as .svg files which were further manipulated in INKSCAPE 0.48.4 (http://inkscape.org) to generate Figures 6 and 7.

RESULTS AND DISCUSSION

Marinobacter hydrocarbonoclasticus SP17 forms oleolytic biofilms on various hydrophobic organic compounds

M. hydrocarbonoclasticus SP17 was previously shown to be able to degrade a wide range of medium-chain *n*-alkanes (C_8 to C_{28}) and two *n*-alkanols (C_{12} and C_{16}) through the formation of a biofilm at the HOC-water interface (Klein *et al*. 2008). In order to further define the substrate range of this strain, biofilm formation was tested on a wider range of HOCs provided as the sole source of carbon and energy (Table 1; Figure 1). Biofilm growth was observed either on liquid or solid, saturated or unsaturated aliphatic compounds such as medium-chain alkanes, alkenes, fatty alcohols and acids, triglycerides or wax esters. Although *M. hydrocarbonoclasticus* SP17 was initially recognized as a marine hydrocarbonoclastic bacterium and thus considered as playing an important role in hydrocarbon degradation (Gauthier *et al*., 1992; Yakimov *et al*., 2007), its wide metabolic capacity indicates that it should rather be considered as a versatile degrader of oily organic substrates. As such, we propose to refer to *M. hydrocarbonoclasticus* SP17 biofilm as an oleolytic biofilm. Its ability to grow as a biofilm on a wide range of poorly soluble HOCs make this bacterium well adapted to the recycling of particulate hydrophobic organic carbon in the ocean (Volkman & Tanoue, 2002; Azam & Malfatti, 2007).

Biofilm formation on *n*-hexadecane or triolein involves different genetic programs

Considering the variety of physical and chemical nature of the HOC-water interfaces tested in Table 1, we wondered whether specific cellular processes are involved in the recognition of the nutritive status of the interface, the adhesion to the interface and the catabolic pathways that sustain substrate assimilation and biofilm growth on the different HOCs. A transcriptomic study using a microarray chip carrying the whole genome of *M. hydrocarbonoclasticus SP17* was performed in order to identify genes regulated in response to biofilm formation on the alkane *n*-hexadecane and the unsaturated triglyceride triolein. These two compounds were chosen because they are representative of two substrate classes that *M. hydrocarbonoclasticus* SP17 may degrade in the environment, *i.e.* hydrocarbons of anthropogenic or biological origin and biogenic lipids. The expression profiles of the whole set of *M. hydrocarbonoclasticus* SP17 genes were measured in cells from 24h-biofilms formed at the water-HOC interfaces and from planktonic cells growing exponentially on acetate. Microscopic observations on samples obtained with *M. hydrocarbonoclasticus* MJ6-1 fluorescent cells grown in the same conditions confirmed that mature biofilms were produced onto both kinds of HOCs in these conditions (Figure 2). Gene expression levels in these three conditions were then compared to each other (Supplemental Table 1).

A total of 1,219 genes out of the 3,839 that were identified as differentially expressed in biofilm cells growing on at least one of the HOC interface (Figure 3; Supplemental Table 2) in comparison to cells growing exponentially on acetate (significant FDR(BH) p-val < 0.05). The high number of genes displaying altered expression during biofilm formation is indicative of dynamic regulatory mechanisms underlying this growth process. Six expression categories belonging to three groups of genes were defined according to relative gene expression levels in the three culture conditions (Figure 3): genes over-expressed (HEX^+ category, 66 genes) or down-expressed (TRI^+AC^+ category, 137 genes) in biofilms on *n*-hexadecane belonged to the

BF HEX group, genes over-expressed (TRI^+, 451 genes) or down-expressed (HEX^+AC^+, 441 genes) in biofilms on triolein belonged to the BF TRI group, and genes over-expressed (HEX^+TRI^+, 75 genes) or down-expressed (AC^+, 145 genes) in biofilm conditions belonged to the BF COM group (Supplemental Table 2). These results also confirm that biofilm growth on either HOCs involved distinct genetic responses together with a core of common genes that might play in general mechanisms of biofilm formation on any HOC. One striking result is the large difference in the numbers of genes affected between the two HOCs substrates. Although being assimilated by *M. hydrocarbonoclasticus* SP17 through a common biofilm lifestyle, to grow as a biofilm on *n*-hexadecane may require less adaptation than on triolein when compared to exponential growth on acetate. Hexadecane may present to bacterial cells an interface with different chemo-physical properties or nutrient status in comparison to triolein that are somewhat easier to grow on. Another reason could be associated to the numerous sources of triglycerides that exist in the marine environment where they can be found for instance in cell debris, or as oil bodies, organelles or membranes in living vegetal, animal or prokaryotic cells. One could therefore consider that forming a biofilm on triolein may signify for the bacterial cells to modulate a larger panel of biological processes.

Biofilm growth on triolein strongly reduces primary metabolism and genetic information processing

Considering the large differences in gene number observed between BF TRI and BF HEX groups, we wondered whether these differences could correspond to the modulation of specific biological processes. The BF TRI, BF HEX and BF COM genes were mapped into the KEGG pathway resource using the annotated *M. hydrocarbonoclasticus* SP17 genome provided in the KEGG genome database (Kanehisa *et al.*, 2013). The KEGG pathway module generated lists of annotation terms that were then classified into biological processes and

represented in relationships with their expression profiles (Figure 4). However, as only 51, 63 and 271 genes could be mapped from the BF HEX, BF COM and BF TRI groups, respectively, these results could only allow a partial interpretation of the larger datasets available from the transcriptomic results (Supplemental Table 3).

The main observation that came out concerns the high proportion of terms that annotated down-regulated genes in biofilms on triolein. Indeed, while down-regulated genes provided 55% and 58% of the annotation terms in the BF HEX and BF COM groups, respectively, they provided 82% of the annotations in the BF TRI group.

The biological processes whose expression seemed to respond significantly to biofilm growth on triolein were carbon and energy metabolism and genetic information processing. More particularly, carbohydrate metabolism (tricarboxylic cycle and glyoxylate shunt, glyoxylate metabolism, glycolysis, 2-oxocarboxylic acid metabolism), fatty acid biosynthesis and degradation, nucleotide and amino acid metabolism were over-represented in the annotated down-expressed genes (Figure 4; Supplemental Table 3). Furthermore, 45 genes coding for the ribosomal proteins (21 small subunit genes and 24 large subunit genes) were also significantly down expressed, together with genes involved in transcription, translation and protein fate. Taken together, these results might signify that a major part of the cells enclosed in biofilm on triolein were less metabolically active than those on *n*-hexadecane or growing exponentially on acetate. However, as suggested earlier, considering that 390 of the 451 genes over-expressed in biofilms on triolein were not mapped on KEGG pathways, with 347 of them coding putative functions (76 genes), conserved hypothetical proteins (158 genes) or unknown proteins (113 genes), one can hypothesize that biofilm growth on triolein involves biological processes that are still to be characterized.

Gene expression in biofilms on *n*-hexadecane confirmed a role for proteins involved in alkane assimilation and type VI secretion system

Genes involved in the primary steps of alkane oxidation provide one example of substrate-specific genes that are overexpressed only in biofilms on *n*-hexadecane. One gene encoding a terminal-1-alkane monooxygenase (MARHY2735) homologous to AlkM and a cluster of three genes expressing a cytochrome P450 alkane hydroxylase (MARHY2838, homologous to AhpG2), an alcohol dehydrogenase homologous to AlkJ (MARHY2839) and a ferredoxin (MARHY2837) are among the most over-expressed genes in this condition, with no significant differential expression on triolein in comparison to acetate. Consistent with gene expression studies carried out on alkane biodegradation pathways in bacteria, this induction of alkane oxidation genes was expected (Rojo, 2009; Sabirova *et al*., 2011). In contrast, *MARHY3758*, which is orthologous to *almA*, a flavin-binding monooxygenase gene involved in long-chain hydrocarbon (>32 carbons) degradation in *Acinetobacter* and *Alcanivorax* species, showed no change in expression (Wang & Shao, 2012). This carbon-chain length specificity confirms that the transcriptomic results are relevant to the experimental culture conditions.

Interestingly, other genes belonging to this HEX^+ category also confirmed notable results obtained from a previous proteomic study carried on *M. hydrocarbonoclasticus* SP17 biofilms grown on *n*-hexadecane (Vaysse *et al*., 2009). For instance, five genes showing specific and significant over-expression on *n*-hexadecane produce proteins that had been described as being among the most abundant proteins detected in biofilms on *n*-hexadecane. The *MARHY2686* gene encodes a protein that was the most abundant in this conditon. Interestingly, it forms a putative operon with two other genes (*MARHY2685* and *MARHY2687*) that showed the same specific HEX^+ expression pattern (Supplemental Table 2). The four other genes are *MARHY3634* and *MARHY3635*, two members of a type VI

secretion system (T6SS) gene cluster, and *MARHY0478* and *MARHY0477* genes which present reduced hydrocarbon assimilation when mutated (Mounier, 2013). Such a consistent pattern of expression from two independent experimental strategies together with mutant phenotypes reinforce the likelihood for a role of these proteins in biofilm growth on that particular HOC.

Chemotaxis and motility genes are down-regulated in biofilm conditions

Among the 130 genes annotated as being involved in chemotaxis and motility, 57 were differentially expressed in biofilm conditions with 70% of them being down-regulated (Supplemental Table 4). The main processes that were affected concern the chemosensory signaling pathways, type IV and MSHA pili formation and, to a lesser extent flagellar assembly (Figure 5).

Chemotaxis controls motility apparatus such as pili or flagella to migrate towards favorable or outwards detrimental environments. It is mediated by chemoreceptors which sense chemo-effectors by a specific receptor-ligand interaction that in turn activates intracellular signaling cascades to control cell movements (Krell *et al*., 2011; Porter *et al*. 2011). The transcriptomic data show that the expression of a large majority of the proteins of the chemosensory signaling cascades which control flagellum assembly and rotation (CheA/CheW) and pili-dependent twitching motility (ChpA/PilJ) was reduced during *M. hydrocarbonoclasticus* SP17 biofilm growth on HOCs (Figure 5A).

Biofilm formation on HOCs also affected the expression of flagellum genes, although to a lower extent than chemotaxis or pili genes. Indeed, even though more than 50 *M. hydrocarbonoclasticus* SP17 genes were annotated as being involved in flagellum assembly and rotation, only a putative *fliD* (*MARHY2507*) was specifically down-expressed in biofilms on *n*-hexadecane. Six genes, *i.e. fliC*, *fliE*, *flgF*, *motA*, *flhB* and a putative *flgL* (*MARH2170*),

were affected in their expression in biofilm conditions on both HOCs (BF COM group), the three former being over-expressed whereas the three latter were down-expressed. Biofilm growth on triolein modulated specifically the expression of *fliM*, *fliQ*, *flhF*, *flgG*, *flgD*, *flgC* and *fgtA*. All were down-expressed but *fliQ*. Interestingly, all these genes correspond mainly to the late expressed genes that are involved in the export and the assembly of the rod, hook and filament parts of the flagellum. Flagella have been involved in different steps of biofilm formation in many bacterial species such as cell swimming to attractive surfaces, cell sticking and swarming on surfaces and cell detachment (Sauer *et al*., 2004; Conrad, 2012; Friedlander *et al*. 2013; Partridge & Harshey 2013). Consistently, flagellum motility is regulated during biofilm formation (Guttenplan & Kearns, 2013). Taken together, the results we have obtained on both chemotaxis and flagellum assembly genes indicate that, at the time of sample collection during that particular experiment, *M. hydrocarbonoclasticus* SP17 cells embedded in biofilms on HOCs did no longer need flagellum-mediated motility. Flagella and chemotaxis have been shown to play a role in biofilm formation in *Marinobacter adhaerens* since the *cheA*, *cheB*, *chpA* or *chpB* mutants are impaired in biofilm formation on abiotic surfaces (Sonnenschein *et al*., 2012). Moreover, we showed that *M. adhaerens* formed biofilms on paraffin while the *fliC* and *fliA* flagella mutants did not (unpublished results).

Type-IV pili genes form clusters that are conserved across Proteobacteria phylum at different loci (Pelicic, 2008). The mapping of expression data in four clusters of type IV pili genes of the *M. hydrocarbonoclasticus* SP17 genome showed that down-regulation of gene expression was not restricted to individual genes but rather concerned gene clusters, thus suggesting a co-regulation process aimed at reducing the role of the whole pili-mediated processes. In particular, two pili gene clusters, *i.e. pilMNOPQ* and *pilVWXY1* are down-expressed in biofilms either on *n*-hexadecane or triolein (Figure 5B). As for flagellum genes, biofilm growth seemed to mainly regulate pili assembly genes. *M. hydrocarbonoclasticus* SP17

biofilm cells are then expected to have a reduced amount of these two extracellular motility structures. Such a down-expression of pili biogenesis genes was also described in *A. borkumensis* growing on *n*-hexadecane (Sabirova *et al*., 2011), although it concerned only four genes. Nevertheless, our study and the large number of genes affected could confirm that type IV pili down-expression might be considered as a characteristic feature of marine hydrocarbonoclastic bacteria growing at water-HOC interfaces. However, considering the variety of pilin sequences and roles, it is difficult to give a hypothesis on the exact significance of such a down-expression in mature biofilms on HOCs.

Marinobacter hydrocarbonoclasticus SP17 genome also contains a characteristic single large cluster of genes encoding a mannose-sensitive haemagglutinin (MSHA) pilus, a type IV pilus found in *Vibrio cholerae* and other environmental bacteria (Marsh & Taylor, 1999; Thormann *et al*., 2004; Boyd *et al*., 2008; Saville *et al*., 2010). This MSHA pilus system has been involved in the adhesion of cells and biofilm formation onto a variety of abiotic and biotic surfaces such as glass (Thormann *et al*., 2004), chitin (Shime-Hattori *et al*., 2006), the cellulose-containing surface of the green alga *Ulva australis* (Dalisay *et al*., 2006) and zooplankton (Chiavelli *et al*., 2001). It is therefore of interest to note that up to ten genes out of the 16 that form this cluster were down-regulated in biofilm conditions, with for instance *mshA* that encodes the major pilin subunit.

The role of MSHA and type IV pili in promoting adherence to surfaces, cell aggregation and biofilm formation is well documented (Giltner *et al*., 2012). Our results show that they may also mediate biofilm formation at HOC-water interfaces. As a down-expression in biofilm conditions signifies that these genes are rather over-expressed in planktonic cells growing on acetate, one can consider that their functions were in fact less necessary in biofilms. This could support the hypothesis that they might be involved in the detection of and the adhesion to HOC-water interfaces. A validation of such hypothesis would be of great interest as it

would indeed put forward potential targets for future studies on HOC-water interfaces colonization in relationship with carbon recycling in the marine environment or hydrocarbon bioremediation in polluted areas.

Biofilm growth on triolein induces the transcriptional activation of a putative 150 kb-genomic island

All the differentially expressed genes were mapped onto the genome of *M. hydrocarbonoclasticus* SP17 in relationship with their expression profiles (Figure 6). This graphical representation revealed that most of the genes that showed overexpression on triolein (TRI^+ and TRI^+AC^+ categories) clustered in eight regions of the genome. On the other hand, very few genes overexpressed on *n*-hexadecane mapped to these regions. In particular, it pointed to a 168-kb genomic region located approximately between positions 1,877,000 and 2,045,000 (from *MARHY1803* to *MARHY2007*)(Grimaud *et al*., 2012), which will be further referred to as the 2-Mb region. For instance, 123 out of the 203 genes of this 2-Mb region belonged to the TRI^+ category, *i.e.* genes specifically over-expressed in biofilm on triolein. This high density of similarly expressed genes at the same locus hinted the presence of a putative genomic island (GI). GIs are large (usually >8 kb) mobile genetic elements that are horizontally transferred between bacteria. They generally convey genetic information that influences traits such as pathogenicity, resistance to antibiotics and toxic compounds, symbiosis, fitness, and adaptation (Dobrindt *et al*., 2004). Acquisition of GIs by bacteria is thought to provide genetic flexibility, more particularly in environmental micro-organisms, that may be subjected to constant environmental changes. A recent study have roughly estimated that more than 90% of the marine bacteria across the four major prokaryotic taxa in the oceans carry GIs in their genomes (Fernández-Gómez *et al*., 2012).

We first took advantage of the development of bioinformatics tools to test the presence of a GI in the 2-MB region (Langille *et al*., 2010). Since bacteria gain GIs through horizontal gene transfer and can even lose it sporadically, the phyletic patterns of the GI and the host genomes may differ. We thus performed a genome comparative analysis between the *M. hydrocarbonoclasticus* SP17 and VT8 strains using the MAUVE whole-genome sequence alignment tool (Figure 7)(Darling *et al*., 2004; Márquez & Ventosa, 2005). This comparison confirmed that a region starting at position 1,927,665 (end of *MARH1950*) and ending at position 2,031,430 (between *MARHY1992* and *MARHY1993*) was absent of *M. hydrocarbonoclasticus* VT8 genome while the whole core genome of *M. hydrocarbonoclasticus* SP17 was conserved (LCB weight of 7060). Moreover, this region was also predicted as being a putative GI by the IslandViewer tool which combines three independent and accurate methods, that is IslandPath-Dimob, SIGI-HMM and IslandPick, which are based on sequence-composition and comparative-genome based analyses (Figure 6)(Dhillon *et al*., 2013). Islandviewer predicted the presence of 18 putative GIs in *M. hydrocarbonoclasticus* SP17 genome (Supplemental Table 5). In particular, it delineated three close putative GIs in the 2-Mb region, between positions 1,926,444 (*MARHY1848*) and 2,032,417 (*MARHY1993*) on the genome. A large part of this zone was identified by all three methods, thus reinforcing its prediction. As underlined by the IslandPath-DIMOB program, this region presented both a strong bias in GC% content in comparison to flanking genomic regions and the presence of 10 genes of the “mobile and extra-chromosomal elements” COG annotation category, within which were four transposases, three putative integrases, one resolvase and one reverse transcriptase genes. Another interesting feature that is commonly associated with GIs is the high percentage of genes of unknown function, a percentage that is about 55% in the 2-Mb region. This proportion is in accordance with percentages found in GIs in other marine bacteria (Fernández-Gómez *et al*., 2012). Together with other features

such the presence of a tRNA gene close to the GI insertion site (*MARHYTRNA25-LEU* at position 1,885,807, between *MARHY1810* and *MARHY1811*) and flanking direct repeats (not shown), all these genomic data provide some confidence that this particular region is probably a GI.

The relationship that exists between the overexpression of half of the genes of this 2-Mb region, other putative mobile elements and biofilm growth on triolein is unclear, in particular whether this corresponds to the production of proteins involved in biofilm formation. This relationship is even more difficult to find out as 86 out of the 137 differentially expressed genes have no known function. Furthermore, no clear bioprocess likely involved in biofilm formation emerges from gene annotation data, although functional categories seem conserved with other marine Gammaproteobacteria GIs (Fernández-Gómez *et al*., 2012). Nevertheless, a cluster of genes, (*MARHY1837* to *MARH1843*) is of particular interest as it concerns the biosynthesis of glycogen-like alpha-glucan polysaccharides metabolism. A similar cluster of genes in *E. coli* (*glgBXCAP*) together with *glgS* were involved in glycogen biosynthesis. Interestingly, *E. coli* Δ*glgS* mutant cells produced less glycogen, were hyperflagellated and hyperfimbriated, displayed elevated swarming motility and an increased ability to form biofilms on polystyrene surfaces, suggesting a link between glycogen production and biofilm formation (Rahimpour *et al*., 2013).

The overexpression of this 2-Mb region could point to a more general response that would link biofilm growth on triolein and transcriptional activation of mobile DNA elements. Indeed, beside this 2-Mb region, a careful analysis of the results presented in Figure 6 shows that there seems to exist a systematic co-localization between all the IslandViewer predicted-GIs and genes overexpressed in biofilms on triolein. Moreover, consistent with the expression profiles of the DNA mobility genes located within the 2-Mb region, 11 other genes of the same category dispersed within the core genome displayed the same over-expression on

triolein (*MARHY0506* & *MARHY0507*, *MARHY0510*, *MARHY0965*, *MARHY1124* & *MARHY1125*, *MARHY1129*, *MARHY1138* & *MARHY1139*, *MARHY3218*, *MARHY3796*). Among these are three prophage-like genes (*MARHY0506* & *MARHY0507*, *MARHY0510*) that are embedded in a putative Pf1-like prophage (Figure 6). This could suggest a putative role for phage-mediated lysis in *M. hydrocarbonoclasticus* SP17 biofilm dynamics on HOCs. Such a role for prophages in biofilm formation has already been being suggested in other environmental biofilm-forming bacteria. Cell lysis in *Shewanella oneidensis* MR-1 or in *Streptococcus pneumoniae* was shown to release biofilm-promoting factors such as e-DNA to mediate biofilm formation (Carrolo *et al*., 2010; Goedeke *et al*., 2011). Pf4 phage is essential for several stages of the biofilm life cycle of *Pseudomonas aeruginosa* PAO1, more particularly during the dispersal phase which it contributes to by generating the typical hollow centers and cell detachment (Webb *et al*., 2003; Rice *et al*., 2008). The putative role of phage-mediated lysis during *M. hydrocarbonoclasticus* SP17 biofilm formation on HOCs is currently under investigation.

Finally, another attractive hypothesis that could support a link between biofilm growth on triolein and the overexpression of genomic islands is the regulatory link that has been observed between carbon metabolism and virulence in pathogenic strains (for a review see Poncet *et al*., 2009). The presence of specific carbon sources might indicate to bacterial cells that they grow close to putative host cells and that virulence genes are to be regulated. Considering that many of the genomic islands found in bacteria are defined as pathogenic islands as they play a role in virulence (Dobrindt *et al*., 2004), the overexpression of the 2-Mb region might signify that the genetic response observed on triolein is to some extent related to the biological origins of HOCs in marine environment. For instance, marine organisms such as algae are known sources for a large variety of metabolites including HOCs that are further metabolized by heterotrophic bacteria (Qin, 2010). Recently, several bacterial species

specialized in cyclic hydrocarbon degradation were found associated with phytoplankton (Gutierrez *et al*., 2013). Therefore, the presence of triolein could be perceived by *M. hydrocarbonoclasticus* as an indication of the presence of a putative host that would be a source of HOCs.

Acknowledgments

We are grateful to Lidwine Trouilh and Florence Hakil for their expert technical assistance in transcriptomics and molecular biology. J.M. was supported by a PhD fellowship from the french Ministère de l'Enseignement Supérieur et de la Recherche. This work was funded by the french national research agency (ANR) as part of the 2011 "AD'HOC" project and the 6th European Framework Program, Contract 018391 FACEIT.

REFERENCES

Azam F & Malfatti F (2007) Microbial structuring of marine ecosystems. *Nat Rev Microbiol* 5: 782–791.

Benjamini Y & Hochberg Y (1995) Controlling the false discovery rate - a practical and powerful approach. *J Roy Stat Soc B Met* 57: 289–300.

Bolstad BM, Irizarry RA, Åstrand M & Speed TP (2003) A comparison of normalization methods for high density oligonucleotide array data based on variance and bias. *Bioinformatics* 19: 185–193.

Boyd JM, Dacanay A, Knickle LC, Touhami A, Brown LL, Jericho MH, Johnson SC & Reith M (2008) Contribution of type IV pili to the virulence of *Aeromonas salmonicida* subsp. *salmonicida* in atlantic salmon (*Salmo salar* L.). *Infect Immun* 76: 1445–1455.

Carrolo M, Frias MJ, Pinto FR, Melo-Cristino J & Ramirez M (2010) Prophage spontaneous activation promotes DNA release enhancing biofilm formation in *Streptococcus pneumoniae*. *PLoS One* DOI: 10.1371/journal.pone.0015678.

Carver T, Thomson N, Bleasby A, Berriman M & Parkhill J (2009) DNAPlotter: circular and linear interactive genome visualization. *Bioinformatics* 25: 119–120.

Chiavelli DA, Marsh JW & Taylor RK (2001) The mannose-sensitive hemagglutinin of *Vibrio cholerae* promotes adherence to zooplankton. *Appl Environ Microbiol* 67: 3220–3225.

546 Choi KH & Schweizer HP (2006) mini-Tn7 insertion in bacteria with single *att*Tn7 sites:
547 example *Pseudomonas aeruginosa*. *Nat Prot* 1: 153-161.

548 Conrad JC (2012) Physics of bacterial near-surface motility using flagella and type IV pili:
549 implications for biofilm formation. *Res Microbiol* 163: 619–629.

550 Dalisay DS, Webb JS, Scheffel A, Svenson C, James S, Holmstroem C, Egan S & Kjelleberg
551 S (2006) A mannose-sensitive haemagglutinin (MSHA)-like pilus promotes attachment of
552 *Pseudoalteromonas tunicata* cells to the surface of the green alga *Ulva australis*. *Microbiol-*
553 *SGM* 152: 2875–2883.

554 Darling ACE, Mau B, Blattner FR & Perna NT (2004) Mauve: multiple alignment of
555 conserved genomic sequence with rearrangements. *Genome Res* 14: 1394–1403.

556 Dhillon BK, Chiu TA, Laird MR, Langille MGI & Brinkman FSL (2013) IslandViewer
557 update: improved genomic island discovery and visualization. *Nucleic Acids Res* 41: 129–132.

558 Dobrindt U, Hochhut B, Hentschel U & Hacker J (2004) Genomic islands in pathogenic and
559 environmental microorganisms. *Nat Rev Micro* 2: 414–424.

560 Fernández-Gómez B, Fernàndez-Guerra A, Casamayor EO, González JM, Pedrós-Alió C &
561 Acinas SG (2012) Patterns and architecture of genomic islands in marine bacteria. *BMC*
562 *Genomics* 13: 347.

563 Friedlander RS, Vlamakis H, Kim P, Khan M, Kolter R & Aizenberg J (2013) Bacterial
564 flagella explore microscale hummocks and hollows to increase adhesion. *P Natl Acad Sci*
565 *USA* 110: 5624–5629.

566 Gauthier MJ, Lafay B, Christen R, Fernandez L, Acquaviva M, Bonin P, Bertrand JC (1992)
567 *Marinobacter hydrocarbonoclasticus* gen. nov., sp. nov., a new, extremely halotolerant,
568 hydrocarbon-degrading marine bacterium. *Int J Syst Bacteriol* 42: 568–576.

569 Giltner CL, Nguyen Y & Burrows LL (2012) Type IV pilin proteins: versatile molecular
570 modules. *Microbiol Mol Biol R* 76: 740–772.

571 Goedeke J, Paul K, Lassak J & Thormann KM (2011) Phage-induced lysis enhances biofilm
572 formation in *Shewanella oneidensis* MR-1. *ISME J* 5: 613–626.

573 Golyshin PN, Chernikova TN, Abraham WR, Lünsdorf H, Timmis KN & Yakimov MM
574 (2002) Oleiphilaceae fam. nov., to include *Oleiphilus messinensis* gen. nov., sp. nov., a novel
575 marine bacterium that obligately utilizes hydrocarbons. *Int J Syst Evol Micr* 52: 901–911.

576 Grimaud R (2010) Biofilm development at interfaces between hydrophobic organic
577 compounds and water. *Handbook of Hydrocarbon and Lipid Microbiology*, (Timmis KN, ed),
578 pp. 1491-1499. Springer, Berlin/Heidelberg, Germany.

579 Grimaud R *et al*. (2012) Genome sequence of the marine bacterium *Marinobacter*
580 *hydrocarbonoclasticus* SP17, which forms biofilms on hydrophobic organic compounds. *J*
581 *Bacteriol* 194: 3539–3540.

582 Gutierrez T, Green DH, Nichols PD, Whitman WB, Semple KT & Aitken MD (2013)
583 *Polycyclovorans algicola* gen. nov., sp nov., an aromatic-hydrocarbon-degrading marine

584 bacterium found associated with laboratory cultures of marine phytoplankton. *Appl Environ*
585 *Microb* 79: 205–214.

586 Guttenplan SB & Kearns DB (2013) Regulation of flagellar motility during biofilm formation.
587 *FEMS Microbiol Rev* 37: 849–871.

588 Harms H, Smith K & Wick L (2010a) Introduction: Problems of
589 Hydrophobicity/Bioavailability. *Handbook of Hydrocarbon and Lipid Microbiology*, (Timmis
590 KN, ed), pp. 1437–1450. Springer, Berlin/Heidelberg, Germany.

591 Harms H, Smith K & Wick L (2010b) Microorganism-Hydrophobic Compound Interactions.
592 *Handbook of Hydrocarbon and Lipid Microbiology*, (Timmis KN, ed), pp. 1479–1490.
593 Springer, Berlin/Heidelberg, Germany.

594 Irizarry RA, Bolstad BM, Collin F, Cope LM, Hobbs B & Speed TP (2003) Summaries of
595 Affymetrix GeneChip probe level data. *Nucleic Acids Res* 31: e15.

596 Jiménez V, Bravo V & Gutierrez LG (2011) Integral approach for improving the degradation
597 of recalcitrant petrohydrocarbons in a fixed-film reactor. *Water Air Soil Poll* 220: 301–312.

598 Johnsen AR, Wick LY & Harms H (2005) Principles of microbial PAH-degradation in soil.
599 *Environ Pollut* 133: 71–84.

600 Jung J, Noh J & Park W (2011) Physiological and metabolic responses for hexadecane
601 degradation in *Acinetobacter oleivorans* DR1. *J Microbiol* 49: 208–215.

602 Kanehisa M, Goto S, Sato Y, Kawashima M, Furumichi M & Tanabe M (2013) Data,
603 information, knowledge and principle: back to metabolism in KEGG. *Nucleic Acids Res* 42:
604 199–205.

605 Klein B, Grossi V, Bouriat P, Goulas P & Grimaud R (2008) Cytoplasmic wax ester
606 accumulation during biofilm-driven substrate assimilation at the alkane-water interface by
607 *Marinobacter hydrocarbonoclasticus* SP17. *Res Microbiol* 159: 137–144.

608 Krell T, Lacal J, Muñoz-Martínez F, Reyes-Darias JA, Cadirci BH, García-Fontana C &
609 Ramos JL (2011) Diversity at its best: bacterial taxis. *Environ Microbiol* 13: 1115–1124.

610 Langille MGI, Hsiao WWL & Brinkman FSL (2010) Detecting genomic islands using
611 bioinformatics approaches. *Nat Rev Micro* 8: 373–382.

612 Mara K, Decorosi F, Viti C *et al*. (2012) Molecular and phenotypic characterization of
613 Acinetobacter strains able to degrade diesel fuel. *Res Microbiol* 163: 161–172.

614 Márquez MC & Ventosa A (2005) *Marinobacter hydrocarbonoclasticus* Gauthier *et al.* 1992
615 and *Marinobacter aquaeolei* Nguyen *et al.* 1999 are heterotypic synonyms. *Int J Syst Evol*
616 *Micr* 55: 1349–1351.

617 Marsh JW & Taylor RK (1999) Genetic and transcriptional analyses of the *Vibrio cholerae*
618 mannose-sensitive hemagglutinin type 4 pilus gene locus. *J Bacteriol* 181: 1110–1117.

Mounier J (2013) Functional characterization of *Marinobacter hydrocarbonoclasticus* SP17 genes involved in biofilm development on hydrophobic organic compounds. PhD Thesis. Université de Pau et des Pays de l'Adour, Pau, France

Notomista E, Pennacchio F, Cafaro V, Smaldone G, Izzo V, Troncone L, Varcamonti M & Donato A (2011) The marine isolate *Novosphingobium* sp. PP1Y shows specific adaptation to use the aromatic fraction of fuels as the sole carbon and energy source. *Microbial Ecol* 61: 582–594.

Partridge JD & Harshey RM (2013) Swarming: flexible roaming plans. *J Bacteriol* 195: 909–918.

Pelicic V (2008) Type IV pili: *e pluribus unum* ? *Mol Microbiol* 68: 827–837.

Poncet S, Milohanic E, Mazé A *et al*. (2009) Correlations between carbon metabolism and virulence in bacteria. *Contributions to Microbiology, Vol. 16* (Collin M & Schuch R, eds), pp. 88–102. Karger, Basel, Germany.

Porter SL, Wadhams GH & Armitage JP (2011) Signal processing in complex chemotaxis pathways. *Nat Rev Micro* 9: 153–165.

Qin J (2010) Hydrocarbons from algae. *Handbook of Hydrocarbon and Lipid Microbiology*, (Timmis KN, ed), pp. 2818–2825. Springer, Berlin/Heidelberg, Germany.

Rahimpour M, Montero M, Almagro G *et al*. (2013) GlgS, described previously as a glycogen synthesis control protein, negatively regulates motility and biofilm formation in *Escherichia coli*. *Biochem J* 452: 559–573.

Rice SA, Tan CH, Mikkelsen PJ, Kung V, Woo J, Tay M, Hauser A, McDougald D, Webb JS & Kjelleberg S (2008) The biofilm life cycle and virulence of *Pseudomonas aeruginosa* are dependent on a filamentous prophage. *ISME J* 3: 271–282.

Rojo F (2009) Degradation of alkanes by bacteria. *Environ Microbiol* 11: 2477–2490.

Sabirova JS, Becker A, Luensdorf H, Nicaud JM, Timmis KN & Golyshin PN (2011) Transcriptional profiling of the marine oil-degrading bacterium *Alcanivorax borkumensis* during growth on *n*-alkanes. *FEMS Microbiol Lett* 319: 160–168.

Sauer K, Cullen MC, Rickard AH, Zeef LAH, Davies DG & Gilbert P (2004) Characterization of nutrient-induced dispersion in *Pseudomonas aeruginosa* PAO1 biofilm. *J Bacteriol* 186: 7312–7326.

Saville RM, Dieckmann N & Spormann AM (2010) Spatiotemporal activity of the mshA gene system in Shewanella oneidensis MR-1 biofilms. *FEMS Microbiol Lett* 308: 76–83.

Shime-Hattori A, Iida T, Arita M, Park KS, Kodama T & Honda T (2006) Two type IV pili of *Vibrio parahaemolyticus* play different roles in biofilm formation. *FEMS Microbiol Lett* 264: 89–97.

Simon A & Biot E (2010) ANAIS: Analysis of NimbleGen arrays interface. *Bioinformatics* 26: 2468–2469.

Sonnenschein EC, Syit DA, Grossart HP & Ullrich MS (2012) Chemotaxis of *Marinobacter adhaerens* and its impact on attachment to the diatom *Thalassiosira weissflogii*. *Appl Environ Microb* 78: 6900–6907.

Tanaka D, Takashima M, Mizuta A, Tanaka S, Sakatoku A, Nishikawa A, Osawa T, Nogushi M, Aizawa SI & Nakamura S (2010) *Acinetobacter* sp. Ud-4 efficiently degrades both edible and mineral oils: isolation and characterization. *Curr Microbiol* 60: 203–209.

Thormann KM, Saville RM, Shukla S, Pelletier DA & Spormann AM (2004) Initial phases of biofilm formation in *Shewanella oneidensis* MR-1. *J Bacteriol* 186: 8096–8104.

Tribelli PM, Martino CD, López NI & Iustman LJR (2012) Biofilm lifestyle enhances diesel bioremediation and biosurfactant production in the Antarctic polyhydroxyalkanoate producer *Pseudomonas extremaustralis*. *Biodegradation* 23: 645–651.

Vaysse PJ, Prat L, Mangenot S, Cruveiller S, Goulas P & Grimaud R (2009) Proteomic analysis of *Marinobacter hydrocarbonoclasticus* SP17 biofilm formation at the alkane-water interface reveals novel proteins and cellular processes involved in hexadecane assimilation. *Res Microbiol* 160: 829–837.

Volkman JK & Tanoue E (2002) Chemical and biological studies of particulate organic matter in the ocean. *J Oceanogr* 58: 265–279.

Wakeham SG, Lee C, Hedges JI, Hernes PJ & Peterson ML (1997) Molecular indicators of diagenetic status in marine organic matter. *Geochim Cosmochim Ac* 61: 5363–5369.

Wang W & Shao Z (2012) Diversity of flavin-binding monooxygenase genes (almA) in marine bacteria capable of degradation long-chain alkanes. *FEMS Microbiol Ecol* 80: 523–533.

Webb JS, Thompson LS, James S, Charlton T, Tolker-Nielsen T, Koch B, Givskov M & Kjelleberg S (2003) Cell death in *Pseudomonas aeruginosa* biofilm development. *J Bacteriol* 185: 4585–4592.

Yakimov MM, Timmis KN & Golyshin PN (2007) Obligate oil-degrading marine bacteria. *Curr Opin Biotech* 18: 257–266.

Yoshimura K & Hama T (2012) Degradation and dissolution of zooplanktonic organic matter and lipids in early diagenesis. *J Oceanogr* 68: 205–214.

685 **TABLES**

686

687 Table 1: Biofilm growth ability of *M. hydrocarbonoclasticus* SP17 on various hydrophobic

688 organic compounds

Substrates	**Chemical class**	**Final concentration[a]**	**Biofilm growth[b]**
phenyldecane	alkyl-substituted aromatic	0.1 %	+
pristane	branched alkane	0.1 %	-
heptamethylnonane	branched alkane	0.1%	-
methyl-laurate	ester	0.2 %	+++
n-hexadecane	*n*-alkane	0.1 %	+++
n-tetradecane	*n*-alkane	0.1 %	+++
n-dodecane	*n*-alkane	0.2 %	+++
hexadecene	*n*-alkene	0.2 %	+++
1-tetradecene	*n*-alkene	0.2 %	+++
octanol	saturated fatty alcohol	0.1 %	-
Oleic acid	unsaturated fatty acid	0.1 %	+++
triolein	unsaturated triglyceride	0.1 %	+++
eicosane	*n*-alkane	solid	++
dotriacontane	*n*-alkane	solid	-
paraffin	*n*-alkanes	solid	+++
palmitic acid	saturated fatty acid	solid	+++
hexadecan-1-ol	saturated fatty alcohol	solid	+++
tripalmitin	saturated triglyceride	solid	+++
hexadecyl hexadecanoate	wax ester	solid	+++

689 [a] percentages are in v/v; [b] Biofilm growth relates to crystal violet staining intensity. "+++",

690 growth of the same order as those observed on *n*-hexadecane 0.1% or paraffin; "-", no growth.

691

692

693 **FIGURE LEGENDS**

694 **Figure 1: Biofilm growth phenotype of *M. hydrocarbonoclasticus* SP17 on various solid**
695 **HOCs.**

696 Biofilm formation was estimated by crystal violet staining after 20h of growth on a long-chain
697 alkane (dotriacontane, C_{32}) or a mix of long-chain alkanes (paraffin), on a saturated fatty acid
698 (palmitic acid, C_{16}), on a saturated fatty alcohol (*n*-hexadecan-1-ol, C_{16}), on a saturated
699 triglyceride (tripalmitin) and on a wax ester (cetyl palmitate, C_{32}). Growth tests were done in
700 triplicate (rep 1-3). A no-cell control that was initially inoculated with sterile EMS medium
701 shows reference crystal violet staining.

702

703 **Figure 2: Microscopy of *M. hydrocarbonoclasticus* biofilms on *n*-hexadecane and triolein.**
704 *M. hydrocarbonoclasticus* SP17-derived MJ6-1 strain expressing eYFP was grown 35 h in
705 SSW medium supplemented with *n*-hexadecane (a, b) or triolein (c, d) labeled with pyrene.
706 (a) and (c), differential interference contrast (DIC) images of one focus plane showing mature
707 biofilms at the SSW-HOC interface. (b) epifluorescence microscopy of the same focus plane
708 observed in (a) with bacterial cells expressing eYFP (yellow fluorescence) onto *n*-hexadecane
709 (blue fluorescence). (d) structured-illumination epifluorescence microscopy (ApoTome) of the
710 same focus plane observed in (c) with bacterial cells expressing eYFP (yellow fluorescence)
711 onto triolein (blue fluorescence). Bars, 5 μm

712

713 **Figure 3: ‘‘Triangle plot’’ of gene relative expression among the three culture conditions**
714 Each gene is represented by a point whose proximity to each of the substrate-labeled corners
715 reflects the relative expression in that growth condition (see ‘‘Materials and Methods’’ for the
716 numerical formula). Genes expressed in a single condition lie close to a corner, while those

expressed equally in two conditions versus the third one lie close to triangle sides. Genes not significantly biased in any pair-wise comparison (p-val > 0.05) are not shown. Small grey triangles show the position of the main triangle plot in a 1 by 1 by 1 side triangle. Genes of the different expression categories are highlighted as colored open circles: green circles, TRI^+ category; bright green circles, HEX^+AC^+ category; dark blue, AC^+ category; light blue circles, HEX^+TRI^+ category; red circles, HEX^+ category; pink circles, TRI^+AC^+ category.

Figure 4: KEGG pathway mapping of genes differentially expressed in biofilms on *n*-hexadecane and triolein

KEGG annotations from genes of the BF HEX (grey box), BF COM (open box) and BF TRI (black box) groups were classified according to pathway mapping in KEGG pathway/genome database and differential expression ratio (down- or over-expressed in comparison to exponentially acetate growing cells). Numbers refer to the number of KEGG annotation terms in each category.

Figure 5: Differential expression of the chemotaxis and motility genes in biofilms at HOC-water interfaces.

A) Differential expression of the chemosensory system. The regulation of the flagellum assembly and rotation and type IV pili function use similar molecular mechanisms. A histidine kinase (CheA, ChpA) is coupled to a methyl-accepting chemotaxis receptor (MCP, PilJ) by an adaptor protein (CheW, PilI). Upon receipt of a signal, the histidine kinases autophosphorylate and phosphate groups are transferred to response regulators (CheY and CheB; PilG and PilH). Grey triangles in boxes represent down-expression; upper left triangle, *n*-hexadecane condition; bottom right triangle, triolein condition. No over-expression was measured in any biofilm condition.

B) Differential expression of genes in clusters of type IV pili genes. Down-expressed genes are represented as grey open arrows. No over-expression was measured in any biofilm condition.

Figure 6: Mapping of putative genetic features and differentially expressed genes onto *M. hydrocarbonoclasticus* SP17 genome.

M. hydrocarbonoclasticus SP17 genome map was generated with the DNAPlotter Java application of the Artemis genome viewer software. A) The tracks from the outside represent: 1- scale in megabases; 2- forward coding and 3- reverse coding sequences (turquoise blue; black boxes correspond to CDS annotated as mobile and extra-chromosomal elements); 4- GIs prediction by IslandPath-DIMOB (blue box), SIGI-HMM (orange box), IslandPick (green box) and all three methods (red box); 5- location of a putative Pf1-like prophage (position 0.55 Mb) and the 2-Mb region (grey boxes); 6- to 11- genes of the TRI^+, TRI^+AC^+, TRI^+HEX^+, HEX^+, HEX^+AC^+ and AC^+ categories, respectively, with same colors as in Figure 3; 12- %GC plot.

Figure 7: Genome alignment between *M. hydrocarbonoclasticus* SP17 and VT8 strains using MAUVE algorithm

MAUVE progressive alignments between *M. hydrocarbonoclasticus* SP17 and *M. hydrocarbonoclasticus* VT8 defined locally collinear blocks of homologous regions. Homologous regions are indicated by similarly colored blocks and are connected by lines. The boundaries of colored blocks usually indicate the breakpoints of genome rearrangement, unless sequence has been gained or lost in the breakpoint region. The black open box located around the 2-Mb position in the *M. hydrocarbonoclasticus* SP17 genome points to the

putative 2-Mb GI region that has no homologous counterpart in the *M. hydrocarbonoclasticus* VT8 genome.

FIGURES

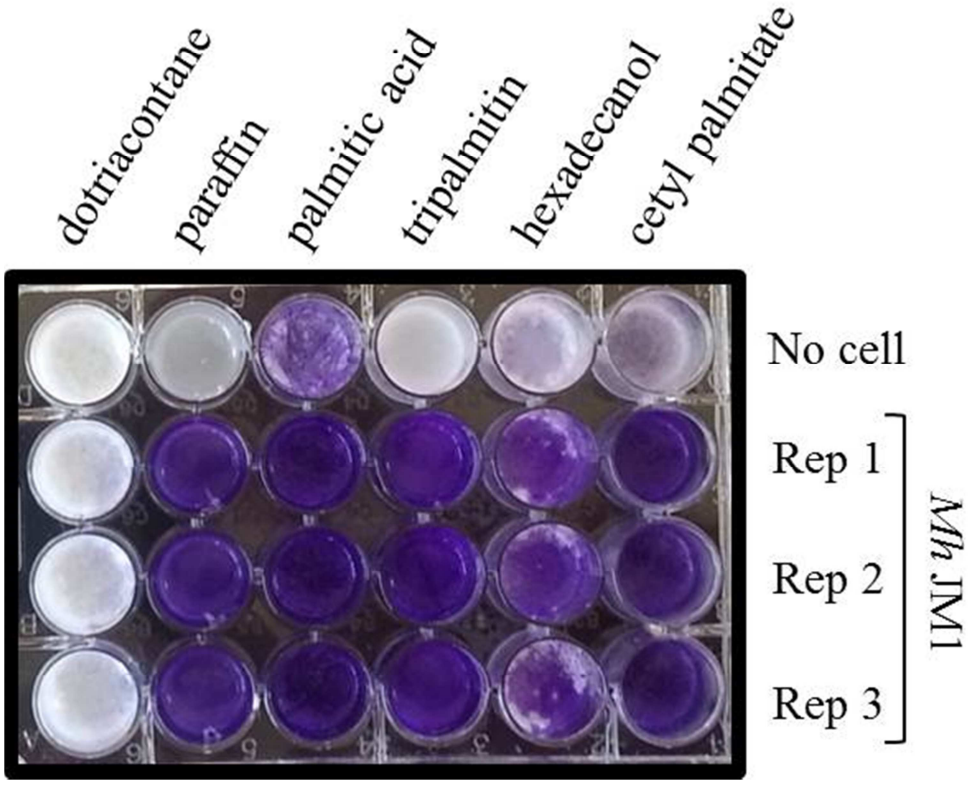

Figure 1

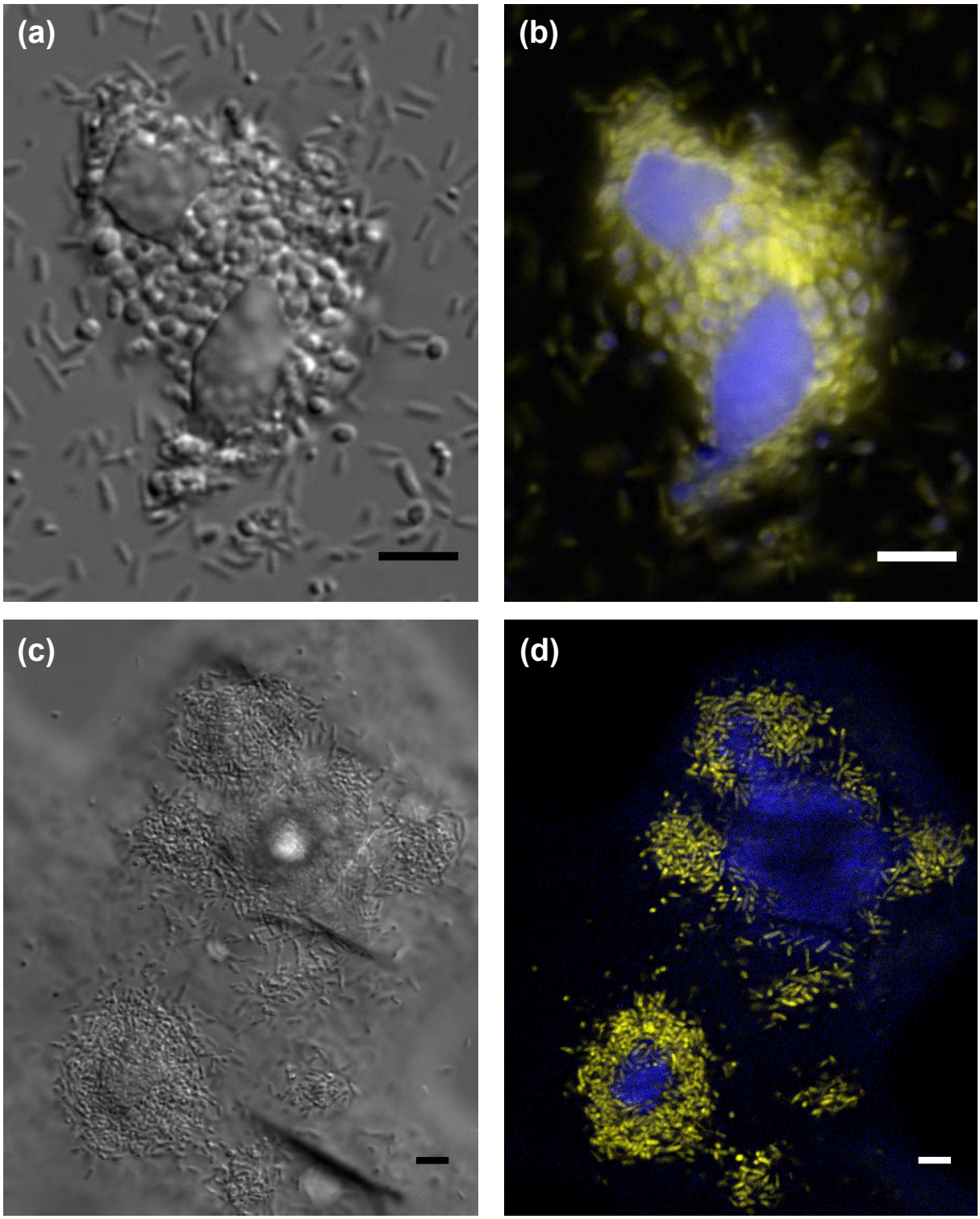

Figure 2

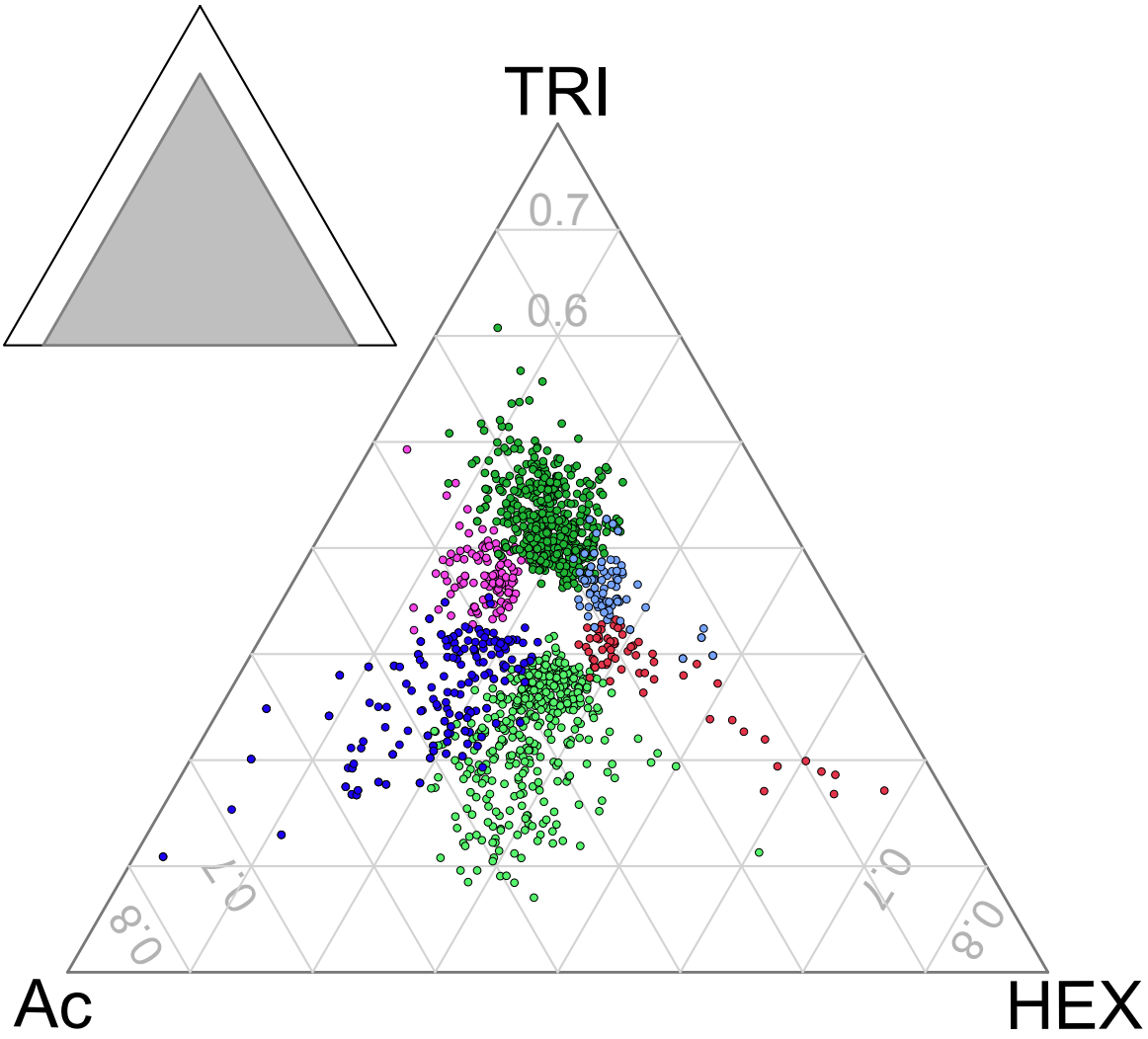

Figure 3

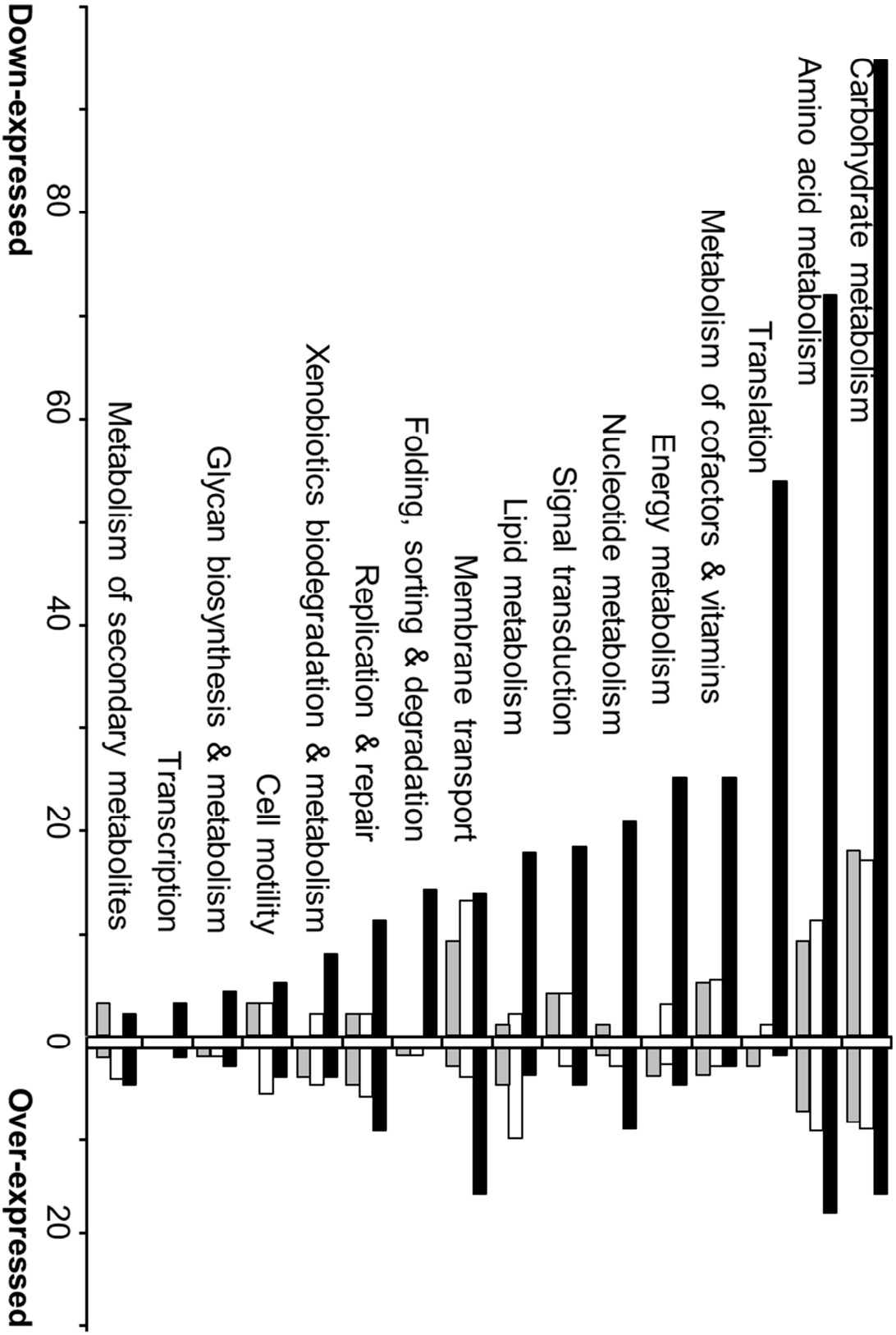
Carbohydrate metabolism
Amino acid metabolism
Translation
Metabolism of cofactors & vitamins
Energy metabolism
Nucleotide metabolism
Signal transduction
Lipid metabolism
Membrane transport
Folding, sorting & degradation
Replication & repair
Xenobiotics biodegradation & metabolism
Cell motility
Glycan biosynthesis & metabolism
Transcription
Metabolism of secondary metabolites
80
60
40
20
0
20
Down-expressed
Over-expressed

Figure 4

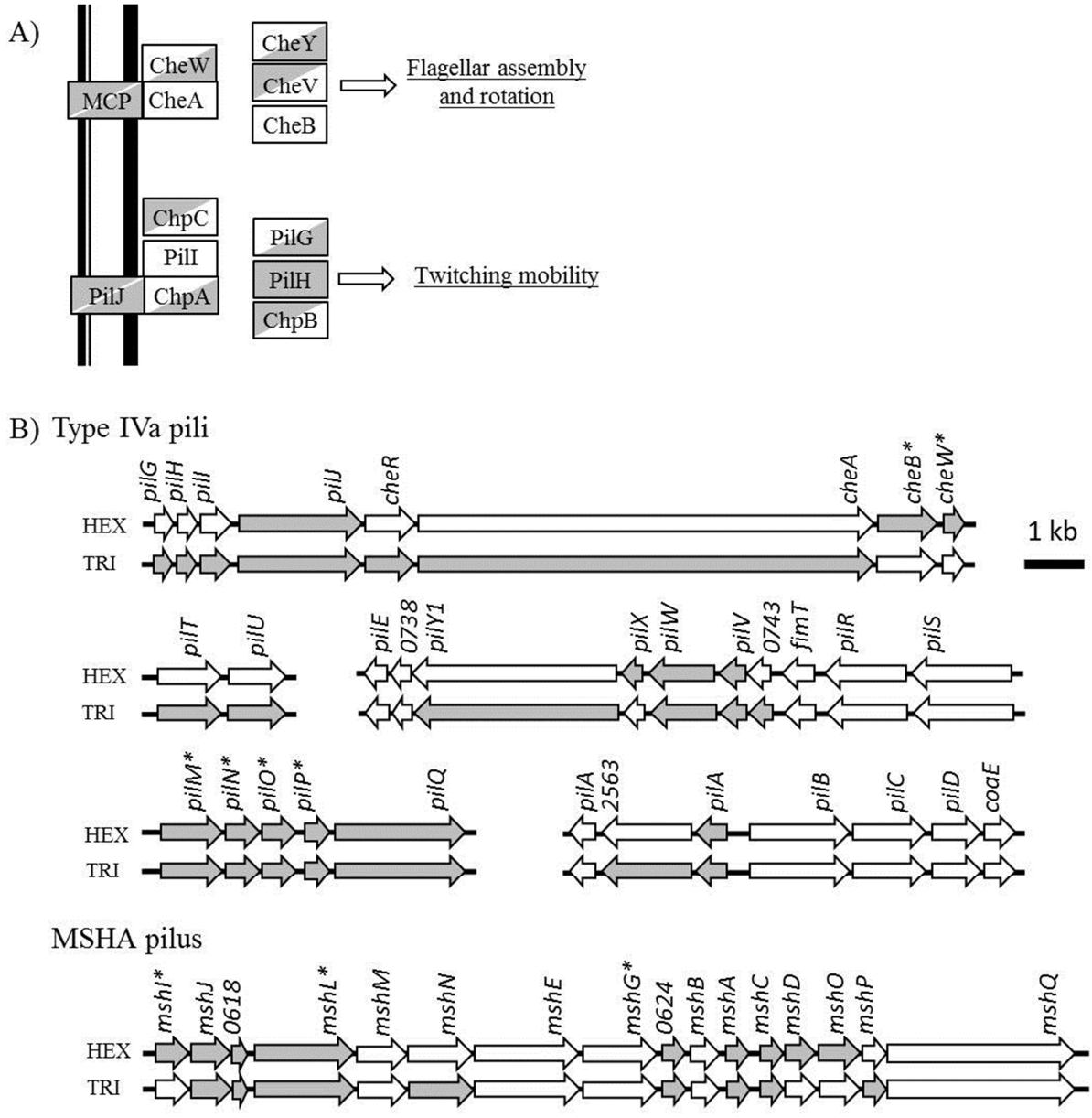
A)
CheW
MCP
CheA
CheY
CheV
CheB
Flagellar assembly and rotation
ChpC
PilI
PilJ
ChpA
PilG
PilH
ChpB
Twitching mobility
B) Type IVa pili
pilG pilH pilI pilJ cheR cheA cheB* cheW*
HEX
TRI
1 kb
pilT pilU pilE 0738 pilY1 pilX pilW pilV 0743 fimT pilR pilS
HEX
TRI
pilM* pilN* pilO* pilP* pilQ pilA 2563 pilA pilB pilC pilD coaE
HEX
TRI
MSHA pilus
mshI* mshJ 0618 mshL* mshM mshN mshE mshG* 0624 mshB mshA mshC mshD mshO mshP mshQ
HEX
TRI

Figure 5

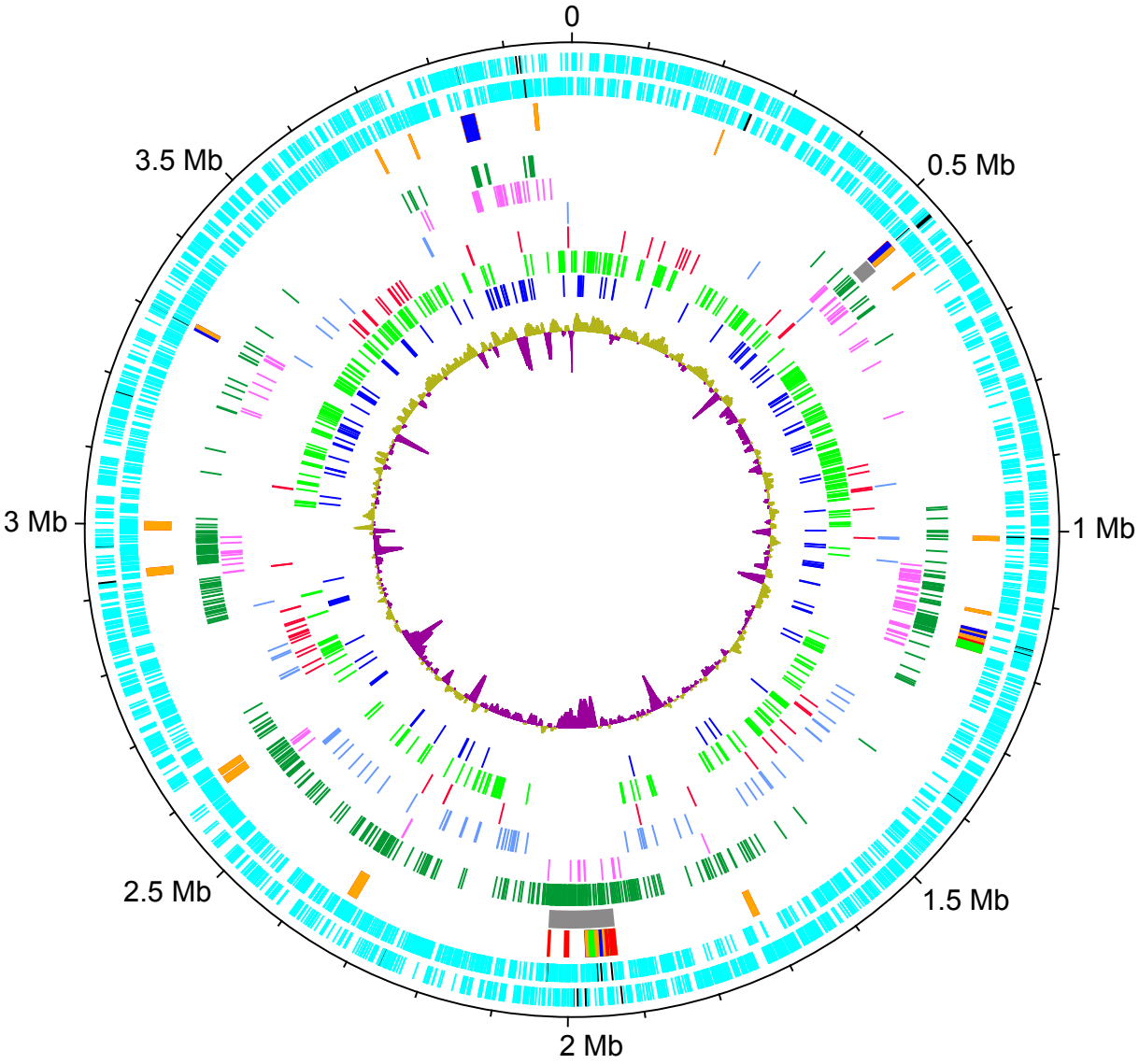

Figure 6

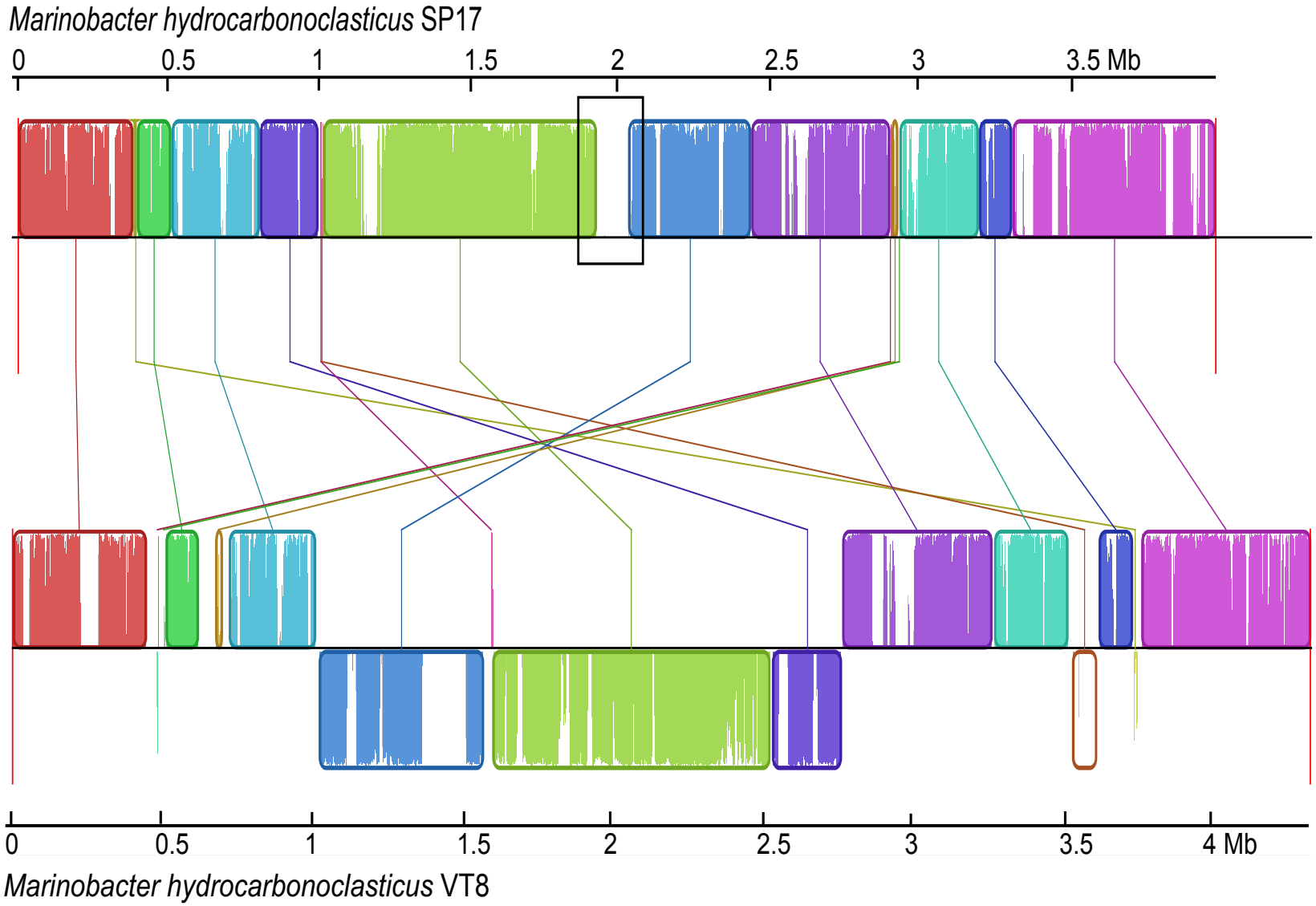
Marinobacter hydrocarbonoclasticus SP17
0
0.5
1
1.5
2
2.5
3
3.5 Mb
0
0.5
1
1.5
2
2.5
3
3.5
4 Mb
Marinobacter hydrocarbonoclasticus VT8

Figure 7